

# Interplay between 2D Antiferromagnetic Correlations and Superconductivity in Oxygen-tuned $\text{La}_{2-x}\text{Ce}_x\text{CuO}_{4\pm\delta}$ Revealed by Ultrafast Optical Spectroscopy

M. C. Wang,<sup>1,2</sup> H. S. Yu,<sup>3</sup> Y. -F. Yang,<sup>3,4</sup> S. N. Luo,<sup>1,2</sup> K. Jin,<sup>3,4,\*</sup> and J. Qi<sup>1,2,†</sup>

<sup>1</sup>*The Peac Institute of Multiscale Sciences, Chengdu, Sichuan 610031, China*

<sup>2</sup>*Key Laboratory of Advanced Technologies of Materials, Ministry of Education, Southwest Jiaotong University, Chengdu, Sichuan 610031, China*

<sup>3</sup>*Beijing National Laboratory for Condensed Matter Physics,*

*Institute of Physics, Chinese Academy of Sciences, Beijing 100190, China*

<sup>4</sup>*Collaborative Innovation Center of Quantum Matter, Beijing, 100190, China*

(Dated: July 27, 2018)

We report on a time-resolved ultrafast optical spectroscopy study of the electron-doped cuprate superconductor  $\text{La}_{2-x}\text{Ce}_x\text{CuO}_{4\pm\delta}$  in a series of oxygen-tuned films with Ce-concentration fixed at optimal doping ( $x = 0.10$ ). We discover that a conspicuous process, emerging at  $\sim 60$  K but disappearing around the superconducting transition temperature, can be attributed to the two-dimensional (2D) antiferromagnetic (AFM) correlations within the  $\text{CuO}_2$  plane. Remarkably, within the investigated oxygen tuning range, the superconducting transition temperature is found to increase linearly with the onset temperature or the effective strength of the 2D AFM correlations. Meanwhile, two gaps associated with the SC order and the 2D AFM correlations have been extracted to be  $2\Delta(0) \sim 9.6$  and  $\Delta_u \sim 125$  meV, respectively. These findings thus help to clarify the intimate relation between 2D AFM correlations and superconductivity in electron-doped cuprates.

Since the discovery of high temperature superconductors (HTSCs), intense research has been focused on unveiling the mechanism of their unconventional Cooper pairing. Specifically, the small isotope effect of optimally doped samples, the superconducting (SC) dome adjacent to an antiferromagnetic (AFM) phase, and the  $d$ -wave SC gap symmetry all shade doubts on the conventional phonon-mediated pairing mechanism [1, 2]. Alternatively, one of the most discussed possibilities is that spin fluctuations may play a vital role in leading to the SC pairing [3, 4]. In contrast to the hole-doped systems, where superconductivity is often intertwined with pseudogap or charge ordering, the electron-doped cuprates are believed to exhibit prominent AFM spin fluctuations [5–10]. Among the electron-doped copper oxides  $\text{R}_{2-x}\text{Ce}_x\text{CuO}_4$  ( $\text{R}=\text{Pr}, \text{Nd}, \text{La}$ ) with optimal Ce-doping, the  $\text{La}_{2-x}\text{Ce}_x\text{CuO}_4$  (LCCO) with  $x \simeq 0.1$  sits in a region closest to the AFM regime in the temperature-doping ( $T$ - $x$ ) phase diagram [5]. Therefore, LCCO should be a good candidate to study the SC order interacting with the AFM correlations. However, relevant investigations are quite rare [11–13]. Powerful techniques such as neutron scattering can be hardly employed, owing to the lack of high quality LCCO single crystals [14]. Therefore, a quantitative relation between the AFM correlations and the superconductivity in LCCO has yet to be established.

In this work, we report the ultrafast optical pump-probe experiments on high quality *oxygen-tuned* LCCO films. The ultrafast optical spectroscopy in time domain has already proved to be quite successful to reveal the interplay between different orders in strongly correlated systems such as HTSCs and heavy fermions [15–19] via monitoring the relaxation of photoexcited quasiparticles coupled to bosons. The oxygen-tuned LCCO films are

critical in this experiment, and provide us unique platforms to investigate the interplay between AFM correlations and superconductivity [7, 9, 10]. By measuring the transient reflectivity change  $\Delta R(t)/R$ , we discover that as temperature decreases a conspicuous quasiparticle relaxation process appears at a characteristic temperature  $T^*$  but vanishes around the SC transition temperature  $T_c$ . Analysis of this prominent feature reveals that such process is associated with the two-dimensional (2D) AFM correlations, whose onset temperature and effective strength are found to depend linearly on the SC transition temperature. These new findings strongly indicate that the 2D AFM correlations are contributive to the superconductivity.

Our time-resolved differential reflectivity  $\Delta R(t)/R$  were measured based on a pump-probe scheme using a Ti:sapphire laser centered at 800 nm ( $\sim 1.55$  eV) with a repetition rate of 80 MHz and a time resolution of  $\sim 35$  fs. The pump fluence was set to a low value of  $\sim 0.15$   $\mu\text{J}/\text{cm}^2$ . The probe intensity was 10 times lower than the pump. The pump and probe beams were cross polarized. Here, we performed all measurements on Ce concentration fixed LCCO films with oxygen finely tuned under zero magnetic field. The four high quality optimal Ce-doped LCCO ( $x=0.1$ ) films with a thickness of 100 nm investigated in this work are: A ( $T_c=18.6$  K), B ( $T_c=25.1$  K), C ( $T_c=23.1$  K) and D ( $T_c=20.6$  K). The oxygen concentration was found to monotonically decrease from A to D. Details of the sample and experimental setup can be found in Refs. [12, 20, 21].

Figure 1(a) shows the typical measured  $\Delta R(t)/R$  in sample B as functions of delay time and temperature, represented by a false color image. We observe three separate temperature regimes where signals behave dis-

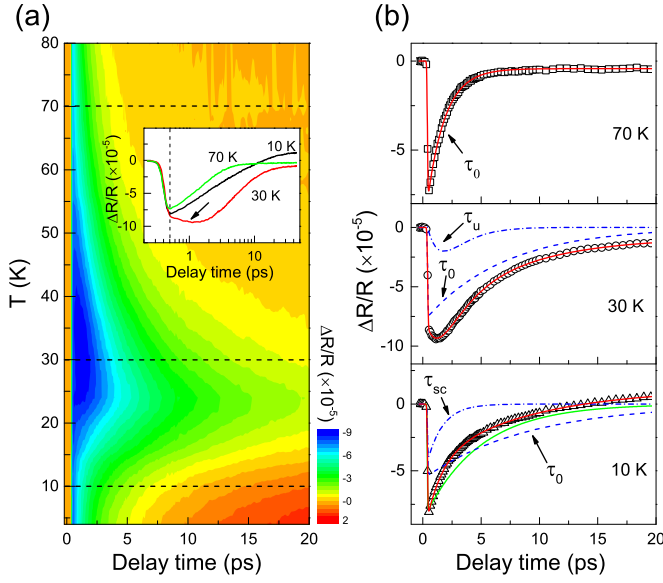


FIG. 1. (color online)  $\Delta R(t)/R$  measurements of sample B ( $T_c=25.1$  K). (a)  $\Delta R(t)/R$  as functions of temperature and time delay displayed in a false color map. Dashed lines represent the signals for three temperatures shown in the inset. The dashed line in the inset indicates the time delay where, at 30 K, the prominent process characterized by  $A_u$  and  $\tau_u$  starts. (b) Red solid lines are the fitting (Eqn. 1) for signals at 70 K (top), 30 K (middle) and 10 K (bottom), respectively. Blue dashed and dash-dotted lines denoted by black arrows show two fitted decay components at 10 K and 30 K, respectively. Green line illustrates the fitting using only one exponential decay at 10 K, and proves the validity of using two exponentials in Eqn. 1 below  $\sim T_c$ .

tinctively. Regime (1): at  $T > T^*$  ( $\simeq 67$  K), signal follows a single exponential decay. Regime (2): in addition to the decay similar with that in regime (1), a peculiar process after initial  $\sim 100$  fs with a timescale of  $\sim 1$  ps emerges below  $T^*$ , but is totally unobserved at  $T \lesssim T^\dagger$  ( $\simeq 23$  K). This process is indicated by the arrow in inset of Fig. 1(a) and the dark blue region in the color map. In fact, within our experimental resolution ( $\pm 3$  K), it is hard to differentiate between  $T^\dagger$  and  $T_c$  for the samples investigated here (similar with what have been reported in Ref. [12]). So for the moment, we assume  $T^\dagger \sim T_c$ . Regime (3): below  $\sim T_c$ , an extra exponential decay is required to describe the observed signals. These three distinct temperature regimes will be more apparent through the fitting procedures. According to these observations, we employ the equations below to fit our experimental data

$$\frac{\Delta R}{R} = \begin{cases} A_0 e^{-t/\tau_0} + C & T > T^*, \\ A_0 e^{-t/\tau_0} + A_u t e^{-t/\tau_u} + C & T^\dagger \sim T_c < T \lesssim T^*, \\ A_0 e^{-t/\tau_0} + A_{sc} e^{-t/\tau_{sc}} + C & T \lesssim T^\dagger \sim T_c. \end{cases} \quad (1)$$

where  $A_j$  ( $j = 0, u, sc$ ) are amplitudes, and  $C$  is a fitting constant. The term characterized by  $A_0$  and  $\tau_0$  persists at all temperatures. The term describing the peculiar

process between  $\sim T_c$  and  $T^*$  is similar with that describing the pseudogap order feature of NCCO in Ref. [17], where, however, the pseudogap order survives far into the SC regime. Therefore, at this stage, we define it as an unidentified order characterized by strength  $A_u$  and decay time  $\tau_u$ . The term characterized by  $A_{sc}$  and  $\tau_{sc}$  only appears below  $\sim T_c$ . It is naturally associated with the SC order. It can be seen that the fitted results are in excellent agreement with the experimental data [Fig. 1(b)], and the corresponding parameters are shown in Fig. 2.

We first address the relaxation process below  $T_c$  characterized by  $A_{sc}$  and  $\tau_{sc}$ , which, as mentioned above, is ascribed to the SC order. Indeed, we observe a divergence of  $\tau_{sc}$  near  $T_c$  [Fig. 2(b)], which is a characteristic behavior observed in many HTSCs [15, 22]. Such phenomenon, associated with a bottleneck effect, is usually attributed to the opening of a SC gap in the density of states, and can be approximated by the Rothwarf-Taylor (RT) model, which describes relaxation of the photoexcited quasiparticles coupled with high frequency bosons [18, 23]. Based on this model, we can extract the density of thermally excited quasiparticles  $n_T(T) \propto \sqrt{\Delta(T)T} e^{-\Delta(T)/T}$  from  $A_{sc}(T)$  (inset of Fig. 2(a)), given by [16, 18]

$$n_T(T) \propto [A_{sc}(T)/A_{sc}(T \rightarrow 0)]^{-1} - 1. \quad (2)$$

For a fixed pump fluence, the  $T$ -dependence of relaxation time  $\tau_{sc}(T)$  is further given by [16, 18]

$$\tau_{sc}^{-1}(T) = \gamma[\beta + 2n_T(T)](\Delta + \alpha T \Delta^4), \quad (3)$$

where  $\alpha$ ,  $\beta$  and  $\gamma$  are fitting parameters. Here,  $\Delta(T)$  is approximated by a BCS-like gap. Fig. 2(a) and (b) demonstrate an excellent agreement between the experimental data and the fitted curves. Our fits to  $A_{sc}$  and  $\tau_{sc}$  yield  $2\Delta(0) = 4.5k_B T_c \simeq 9.6$  meV, which has the same order as that in NCCO ( $2\Delta(0) \sim 8$  meV [24]).

The process characterized by  $A_0$  and  $\tau_0$  persists to high temperatures from SC state to normal state. This decay process, in principle, also represents relaxation of the photoexcited quasiparticles coupled to bosons. However, below  $T_c$  the bosons in this process may not only come from the bottleneck effect as described in the RT model [18, 23], but also can originate from other mechanism, i.e., phonons induced by the coherent Raman excitation [25]. Bosons in the latter case can be excited in normal state at high temperatures. The fact that bosons can be coupled via scatterings may also lead to the relaxation processes characterized by  $A_0$  and  $A_{sc}$  being coupled. These effects are supported by two observations in the experiment. (1) There exists a noticeable peak of  $\tau_0$  around  $T_c$ , the same as that of  $\tau_{sc}$ . (2) When temperature decreases across  $T_c$ , the amplitude  $A_0$  experiences a sudden reduction, while  $A_{sc}$  emerges and grows continuously. Because no clear anomaly around  $T^*$  is observed in  $A_0(T)$  and  $\tau_0(T)$  [see Fig. 2(c)], the processes characterized by  $A_0$  and  $A_u$  should be independent.

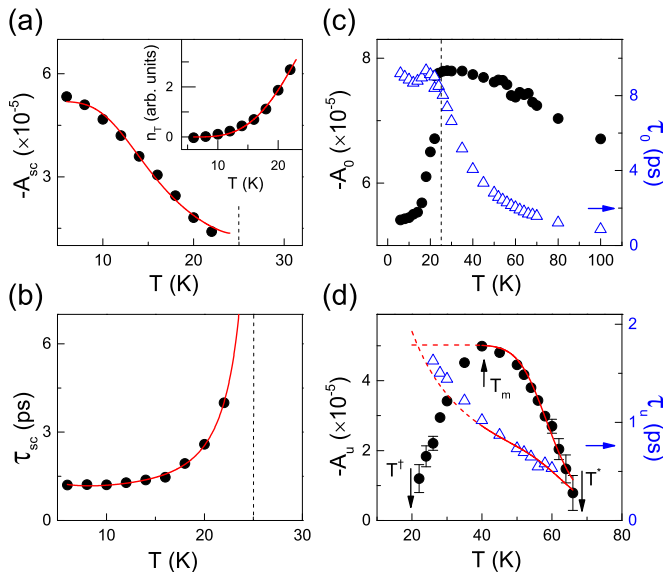


FIG. 2.  $T$ -dependencies of decay time and amplitude for sample B. (a)  $T$ -dependence of  $A_{SC}$ .  $n_T$  extracted from  $A_{SC}$  is plotted in the inset. (b)  $T$ -dependence of  $\tau_{SC}$ . Red solid lines in (a) and (b) are the fitted results using RT model. (c)  $T$ -dependence of  $A_0$  (filled circle) and  $\tau_0$  (open triangle). Dashed lines in (a)-(c) indicate  $T_c$ . (d)  $T$ -dependencies of  $A_u$  (filled circle) and  $\tau_u$  (open triangle). The RT model fits to  $A_u$  and  $\tau_u$  are only for  $T_m < T < T^*$ . The dashed lines are the extrapolation of the fit below  $T_m$ . Black arrows indicate the positions of  $T^*$ ,  $T_m$ , and  $T^\dagger$ , respectively.

We next focus on discussing the process characterized by  $A_u$  and  $\tau_u$ , whose  $T$ -dependencies are shown in Fig. 2(d). It can be seen that the onset temperature  $T^*$  of this process is around 67 K in sample B. Similar characteristic temperature is also observed in a recent pump-probe experiment [13]. We notice that: (1)  $T^*$  coincides with the temperature  $\sim 70(\pm 10)$  K, defining the 2D AFM phase boundary determined by the anisotropic magnetoresistance measurements under an in-plane magnetic field of 14 T [26]; (2)  $T^*$  is close to  $\sim 50(\pm 5)$  K, defining the linear scattering rate boundary associated with the AFM spin fluctuations acquired by  $R$ - $T$  power law investigations under zero field [11]; (3) Three-dimensional AFM order can only exist at a Ce doping level of  $x \leq 0.08$ , revealed by a recent low-energy muon spin rotation experiment [34]. Therefore, these studies strongly suggest that the unidentified order emerging at  $T^*$  should originate from the 2D AFM correlations, whose strength can be characterized by  $A_u$  in our experiments. Fig. 2(d) shows  $A_u$  as a function of temperature. It is clear that as temperature decreases from  $T^*$  to  $T_c$ , strength of this order consecutively increases to a maximum value at  $T_m$  ( $\sim 40$  K), and then decreases. Such extraordinary behaviour implies another mechanism might appear at  $\sim T_m$ , which competes with the 2D AFM correlations characterized by  $A_u$ . A possible explanation is the competition between

the intra-plane and inter-plane AFM couplings [9, 12].

The observation of the 2D AFM correlations in our experiment may further indicate opening of a gap  $\Delta_u$  below  $\sim T^*$  in LCCO. In fact, quite a few studies on electron-doped HTSCs previously reported that a gap could emerge due to the AFM correlations or long-range AFM order above  $T_c$  [27–29]. Therefore, we assume a similar gap,  $\Delta_u$ , opening at  $T^*$ . Using the RT model described above, we can extract this gap by fitting the  $A_u$  and  $\tau_u$  for  $T_m < T < T^*$ . In Fig. 2(d), the excellent agreement between the experimental data and the curve fits confirms our initial expectation of a gap opening. We obtain  $\Delta_u$  with a value of  $\sim 125$  meV, which is consistent with the gaps found above  $T_c$  in NCCO and  $\text{Pr}_{2-x}\text{Ce}_x\text{CuO}_4$  [27, 29].

In order to unravel the detail relationship between 2D AFM correlations and superconductivity, we have carefully investigated the oxygen dependence of the process characterized by  $A_u$ . In fact, this process in all investigated samples behaves very similarly [Fig. 3(a)].  $T^*$ ,  $T_m$ , and  $T^\dagger$  as a function of oxygen concentration are shown in Fig. 3(b). It can be seen clearly that the oxygen concentration dependence of  $T^*$  almost exactly follows that of  $T_c$ , although the exact behaviours of  $T_m$  and  $T^\dagger$  are still not clear due to the limitations of our experimental resolution. Such oxygen-dependence indicates that the 2D AFM correlations may play an important role in establishing the SC order. Further evidences are given by extracting the strength  $A_u$  of 2D AFM correlations [Fig. 3(c)]. In order to obtain the effective strength quantitatively, we employ the average value of  $A_u$  defined by  $\bar{A}_u = \int_{T^\dagger}^{T^*} A_u(T) dT / \int_{T^\dagger}^{T^*} dT$ . The dependence of  $\bar{A}_u$  on  $T_c$  is shown in Fig. 3(d). A nice linear fit of  $\bar{A}_u(T_c)$  strongly supports that 2D AFM spin fluctuations should make a significant contribution to the SC pairing. We note that although  $T^\dagger$  and  $T_c$  are unable to distinguish experimentally, they may have quite different origins [12].

Because as oxygen concentration reduces  $T_c$  of LCCO initially increases and then decreases, the oxygen level of our samples should have spanned in a relatively wide range. It is remarkable that the onset temperature  $T^*$  and the strength  $\bar{A}_u$  of the 2D AFM correlations monotonically increase with  $T_c$  in such a wide range. This finding is in sharp contrast to that observed by varying Ce doping  $x$ , where  $T^*$  can decrease as  $T_c$  increases in underdoped regime [11, 26]. Such big difference may arise from the significant change of electron density (or band filling) induced by varying  $x$ , which contributes to the change of physical parameters measured in the Hall effect measurements [30]. On the contrary, effects due to the change of charge carriers in this work (only oxygen concentration changes) can be largely omitted [29, 31], and hence the variation of  $T_c$  should be mainly attributed to the change in the strength of the 2D AFM correlations.

In fact, because our experiments were performed with-

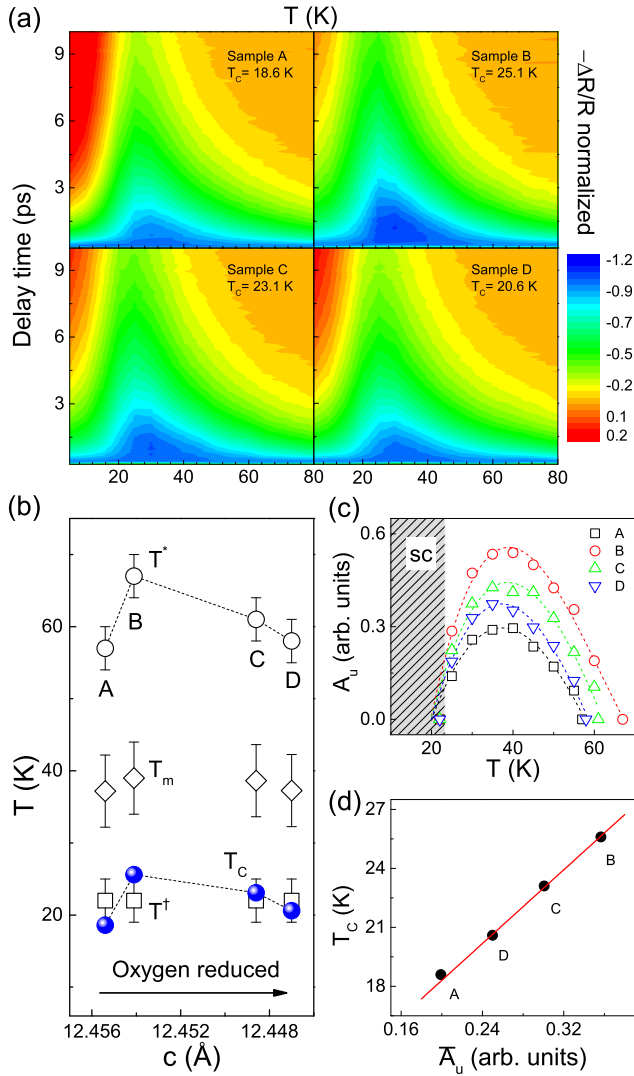


FIG. 3. Oxygen concentration dependence of  $\Delta R(t)/R$ . The oxygen concentration is qualitatively represented by the lattice parameter ( $c$ -axis) [12, 21]. (a)  $\Delta R(t)/R$  data for all samples displayed in the form of false color map. Signals are normalized to the values at the time delay indicated by the dashed line in the inset of Fig. 1(a). (b)  $T^*$  (open circle),  $T_m$  (open diamond),  $T^\dagger$  (open square) and  $T_c$  (sphere) as a function of oxygen concentration. (c) Temperature dependence of normalized  $A_u$  in all samples are plotted together, dashed lines are guides for the eyes. (d)  $T_c$  as a function of  $A_u$  (filled circle), solid line is a linear fit to the data.

out an external magnetic field, our findings thus allow us to clarify some previous inconsistent observations in LCCO that could arise from the slight variation of oxygen [9] or magnetic field-induced effect [32, 33], e.g., low-energy muon spin rotation experiments determined the three-dimensional AFM boundary residing at  $x \sim 0.08$  (close to where superconductivity appears) [34], which is quite different from the value ( $x \sim 0.14$ ) obtained through the upturn in temperature-dependent resistivity measurements under magnetic fields up to 40 T [35].

In summary, we performed time-resolved ultrafast optical spectroscopy experiments on cuprate superconductor LCCO with different oxygen concentrations. We observe a peculiar picosecond quasiparticle relaxation process associated with the 2D AFM correlations at temperatures between  $T^\dagger$  and  $T^*$ . We reveal that both the onset temperature  $T^*$  and the effective strength  $A_u$  of this process increase linearly with the SC transition temperature  $T_c$  as oxygen reduces. Such new findings strongly indicate that 2D AFM spin fluctuations contribute importantly to superconductivity.

This work was supported by China 1000-Young Talents Plan and National Natural Science Foundation of China (Grants No. 11474338).

\* kuijin@aphy.iphy.ac.cn

† jqj@pims.ac.cn

- [1] B. Batlogg et al., Phys. Rev. Lett. **58**, 2333 (1987).
- [2] A. Damascelli, Z. Hussain, and Z.-X. Shen, Rev. Mod. Phys. **75**, 473 (2003).
- [3] J. Rossat-Mignod et al., Physica C **185**, 86 (1991).
- [4] M. R. Norman et al., Phys. Rev. Lett. **79**, 3506 (1997).
- [5] N. P. Armitage, P. Fournier and R. L. Greene, Rev. Mod. Phys. **82**, 2421(2010).
- [6] M. Fujita, M. Matsuda, S. -H. Lee, M. Nakagawa, and K. Yamada, Phys. Rev. Lett **101**, 107003(2008).
- [7] J. Zhao, F. C. Niestemski, S. Kunwar, S. Li, P. Steffens, A. Hiess, H. J. Kang, S. D. Wilson, Z. Wang, P. Dai, and V. Madhavan, Nat. Phys. **7**, 719 (2011).
- [8] D. J. Scalapino, Rev. Mod. Phys. **84**, 1383 (2012).
- [9] H. J. Kang, P. Dai, H. A. Mook, D. N. Argyriou, V. Sikolenko, J. W. Lynn, Y. Kurita, S. Komiya, and Y. Ando, Phys. Rev. B **71**, 214512 (2005).
- [10] S. D. Wilson, P. Dai, S. Li, S. Chi, H. J. Kang, and J. W. Lynn, Nature **442**, 59 (2006).
- [11] K. Jin, N. P. Butch, K. Kirshenbaum, J. Paglione, and R. L. Greene, Nature **476**, 73 (2011).
- [12] H. S. Yu et al., arXiv:1510.07388.
- [13] I. M. Vishik, F. Mahmood, Z. Alpichshev, J. Higgins, R. L. Greene, and N. Gedik, arXiv:1601.06694.
- [14] T. Yamada, K. Kinoshita, and H. Shibata, Jpn. J. Appl. Phys. **33**, L168 (1994).
- [15] V. V. Kabanov, J. Demsar, B. Podobnik, and D. Mihailovic, Phys. Rev. B **59**, 1497 (1999).
- [16] E. E. M. Chia, J. -X. Zhu, D. Talbayev, R. Averitt, A. Taylor, K. -H. Oh, I. -S. Jo, and S. -I. Lee, Phys. Rev. Lett. **99**, 147008 (2007).
- [17] J. P. Hinton, J. D. Koralek, G. Yu, E. M. Motoyama, Y. M. Lu, A. Vishwanath, M. Greven, and J. Orenstein, Phys. Rev. Lett. **110**, 217002 (2013).
- [18] J. Demsar, J. L. Sarrao, and A. J. Taylor, J. Phys. Condens. Matter **18**, R281 (2006); and references therein.
- [19] J. Qi et al., Phys. Rev. Lett. **111**, 057402 (2013).
- [20] M. C. Wang, S. Qiao, Z. Jiang, S. N. Luo, and J. Qi, Phys. Rev. Lett. **116**, 036601 (2016).
- [21] See Supplemental Material for sample details and discussion of the effect due to various pump fluence.
- [22] E. E. M. Chia et al., Phys. Rev. Lett. **104**, 027003 (2010).

- [23] V. V. Kabanov, J. Demsar, and D. Mihailovic, Phys. Rev. Lett. **95**, 147002 (2005).
- [24] T. Sato, T. Kamiyama, T. Takahashi, K. Kurahashi, and K. Yamada, Science **291**, 1517 (2001).
- [25] G. A. Garrett, T. F. Albrecht, J. F. Whitaker, and R. Merlin, Phys. Rev. Lett. **77**, 3661 (1996); R. Merlin, Solid State Comm., **102**, 207 (1997).
- [26] K. Jin, X. Zhang, P. Bach, and R. L. Greene, Phys. Rev. B **80**, 012501 (2009).
- [27] Y. Onose, Y. Taguchi, K. Ishizaka, and Y. Tokura, Phys. Rev. Lett. **87**, 217001 (2001).
- [28] B. Kyung, V. Hankevych, A. -M. Dare, and A. -M. S. Tremblay, Phys. Rev. Lett. **93**, 147004 (2004).
- [29] P. Richard, M. Neupane, Y. -M. Xu, P. Fournier, S. Li, P. Dai, Z. Wang, and H. Ding, Phys. Rev. Lett. **99**, 157002 (2007).
- [30] K. Jin, B. Zhu, B. Wu, L. Gao, and B. Zhao, Phys. Rev. B **78**, 174521 (2008).
- [31] J. Gauthier, S. Gagne, J. Renaud, M. -E. Gosselin, P. Fournier, and P. Richard, Phys. Rev. B **75**, 024424.
- [32] M. Matsuura et al., Phys. Rev. B **68**, 144503 (2003).
- [33] D. Haug et al., Phys. Rev. Lett. **103**, 017001 (2009).
- [34] H. Saadaoui et al., Nature Commun. **6**, 6041 (2015).
- [35] K. Jin et al., Phys. Rev. B **77**, 172503 (2008).